Environmental Science and Pollution Research (2022) 29:49116–49125
https://doi.org/10.1007/s11356-022-19419-0

RESEARCH ARTICLE

High-efficiency stabilization of lead in contaminated soil by thermal-organic acid–activated phosphate rock

Ziwen Song[1,2] · Zhuo Zhang[1,2] · Canyu Luo[1] · Likun Yang[1] · Jin Wu[3]

Received: 12 November 2021 / Accepted: 21 February 2022 / Published online: 25 February 2022

Abstract

Phosphate rock powder (PR) has been shown to possess the potential to stabilize lead (Pb) in soil. Most of the phosphorus (P) minerals in the world are low-grade ores, making it difficult to achieve the expected stabilization effect on heavy metals. This study compared the changes in the phase composition and structure of PR and three kinds of activated phosphate rock powder (APR) (organic acid–activated PR, thermal-activated PR, and thermal-organic acid–activated PR). The stabilization effectiveness of APR on Pb-contaminated soil was evaluated by toxicity leaching procedure; the Pb products adsorbed on APR and stabilization mechanism of APR on Pb were analyzed. The results demonstrated that APR showed decreased crystallinity and 3.4-fold increase in specific surface area, and a 53.07% and 49.32% increase in soluble P content in oxalic acid–activated PR and citric acid–activated PR, respectively, when compared with those of PR. These changes improved the stabilization effect of APR on Pb-contaminated soil, in which oxalic acid-600 °C–activated PR showed the best effect, presenting 94.0–99.8% reduction in Pb leaching concentration following addition of 2–10% modifier. Product characterization after Pb adsorption on APR showed that Pb was adsorbed onto APR by forming fluoropyromophite precipitation with APR.

Keywords Phosphate rock powder · Thermal-organic acid activation · Lead-contaminated soil · Stabilization

Introduction

With rapid urbanization and industrialization, heavy metal contamination of soil has attracted worldwide attention (Yan et al. 2020). With the development of cities, industries, and agriculture, soil contamination is becoming an increasingly severe issue. The increase in the contents of heavy metals, especially lead (Pb), in soil poses a significant threat to the environment and human health (Park et al. 2011). Many industries, including metal processing, mining, electroplating, and battery recycling, can cause Pb pollution. Pb-acid battery recycling plants account for more than 80% of the world's total Pb use and are one of the major sources of Pb pollution (Chowdhury et al. 2021; Gottesfeld et al. 2018; Mignardi et al. 2012). Previous studies have shown that the Pb content in the soil of Pb-acid battery plants could be as high as 10–30%, which poses a high risk owing to the high bioavailable Pb content (Zhang et al. 2015). As Pb is highly toxic and nondegradable, its accumulation in soil and transport through the soil matrix can cause potential hazard to plant growth and human health (Su et al. 2015). Therefore, effective strategies are required to remediate Pb-polluted soil.

Responsible Editor: Kitae Baek.

Highlights

1. Surface area of PRO-600 was 3.4-fold higher than that of PR.
2. Structure of APR changed from agglomerated crystal to a porous structure.
3. Thermal-organic acid–activated PR exhibited better Pb stability than the other two APRs.
4. Leaching concentration of Pb decreased by 99.8% when 10% PRO-600 was added.
5. Pb was adsorbed on APR mainly by forming Pb5(PO4)3F precipitation with APR.

✉ Zhuo Zhang
zzkeren@126.com

[1] School of Land Science and Technology, China University of Geosciences, Beijing 100083, China

[2] Key Laboratory of Land Consolidation and Rehabilitation, Ministry of Natural Resources, Beijing 100035, China

[3] College of Architecture and Civil Engineering, Beijing University of Technology, Beijing 100124, China

Extensive research on remediation technology of soil Pb contamination has been conducted around the world, and remediation techniques such as physical remediation (thermal desorption technology, vitrification technology, etc.), chemical remediation (stabilization remediation technology, electric remediation, etc.), and bioremediation (including microbial remediation, phytoremediation, animal remediation) have been developed. Among them, chemical stabilization has been reported to exhibit advantages such as rapid effect, economic and environment-friendly approach, and wide application scope, being more suitable for remediation of large areas of heavy metals contaminated soil (Awa and Hadibarata 2020, Kumpiene et al. 2008; Mignardi et al. 2012; Yao et al. 2012).

Pb-contaminated soil remediation technology based on phosphorous (P)-containing minerals has been widely studied worldwide. P-containing materials, such as phosphate rock (PR) and hydroxyapatite, can induce the formation of lead phosphate, thereby stabilizing Pb in the soil (Xu et al. 2019). The main benefits of this approach are low cost of P-containing minerals, stability of the products, and possibility of long-term remediation (Jiang et al. 2012). PR is a direct, economical, and lasting source of P (Li et al. 2020), and there are abundant reserves of P minerals around the world. In 2015, the world's P reserves reached 49.75 billion tons, with China ranking second in the world with 13 billion tons of P reserves (Xu et al. 2017). However, most of these resources are low-grade ores from which high phosphate concentrations are difficult to obtain (Xu et al. 2019); hence, direct remediation of heavy metal contamination using PR may make it difficult to achieve the desired effect.

Activation of PR can promote the release of available P from PR and stimulate phytoavailability of P in PR-treated soil by increasing the solubility of PR (Zhu et al. 2015), thus driving the stabilization of Pb in contaminated soil. While current research on PR activation is mainly focused on single treatment method, such as acid activation (Huang et al. 2019; Su et al. 2015) and biological activation (Abbasi and Manzoor 2018, Xu et al. 2019), the combined use of multiple activation methods to activate PR has not been widely investigated, and its remediation effect, application scope, and mechanism on Pb-contaminated soil are not yet clear. Besides, thermal treatment is a common activation method. Studies have been conducted on thermally activated clay minerals (e.g., sepiolite and bentonite) for immobilizing heavy metals in contaminated soils (E.Padilla-Ortega et al. 2020; Zhou et al. 2022). However, thermal activation of PR has not been reported. Therefore, the objectives of the present study were to (1) prepare organic acid–activated PR, thermal-activated PR, and thermal-organic acid–activated PR, (2) discuss the possible stabilization mechanism by analyzing the physical structure and chemical composition of the activated PR (APR), (3) evaluate the stabilization effect of APR on Pb-contaminated soil in a Pb-acid battery plant site through toxicity characteristic leaching procedure (TCLP) method, and (4) provide theoretical basis and technical support for the application of APR in remediation of heavy metals contaminated soil.

Materials and methods

Materials

Soil samples were collected from a Pb-acid battery plant site in Jilin Province, China (128.93° N,43.11° E), then air-dried, crushed, and passed through a 2-mm sieve. The initial pH of the soil samples was 7.61, Pb concentration in the soil samples was 2,861 mg/kg, and TCLP (Toxicity Characteristic Leaching Procedure)-leached concentration of Pb was 7.17 mg/L.

Phosphate rock (PR) used in this study was obtained from Zhongxiang Wangji Phosphate Fertilizer Plant, Hubei Province, China. X-ray fluorescence (XRF) of the PR showed that the main inorganic components of PR were CaO and P_2O_5 (40.49% and 20.09%, respectively), along with trace amounts of Mg, Si, F, Al, and S. All the experimental reagents were purchased from China National Pharmaceutical Group Corporation, and were of analytical grade.

Preparation of activated phosphate rock (APR)

Organic acid activation of PR

For obtaining oxalic acid–activated PR (PRO) and citric acid–activated PR (PRC), 100 g of PR were added to two beakers and respectively mixed with 0.5 mol/L oxalic acid solution and 0.5 mol/L citric acid. Subsequently, the beakers were left at room temperature (25 °C) for 7 days, dried at 60 °C in an oven (Zhang et al. 2018), and the dried PRO and PRC were ground.

Thermal activation of PR

To obtain activated PR at 200 °C (PR200), 400 °C (PR400), and 600 °C (PR600), 100 g of PR was heated in muffle furnace at 200 °C, 400 °C, and 600 °C for 2 h, respectively, and cooled.

Thermal-organic acid activation of PR

For thermal-organic acid activation of PR, 100 g of PR200, PR400, and PR600 were respectively mixed

with 1 L of 0.5 mol/L oxalic acid solution or 1 L of 0.5 mol/L citric acid solution, left at room temperature (25℃) for 7 days, and then dried at 60 °C in an oven. Subsequently, the dried thermal-organic acid–activated PR were ground to obtain oxalic acid-200 °C–activated PR (PRO-200), oxalic acid-400 °C–activated PR (PRO-400), oxalic acid-600 °C–activated PR (PRO-600), citric acid-200 °C–activated PR (PRC-200), citric acid-400 °C–activated PR (PRC-400), and citric acid-600 °C–activated PR (PRC-600).

Stabilization of Pb-contaminated soil

In a beaker containing 30 g of dried and sieved soil samples, PR/APR were added at the ratios of 2%, 5%, 7%, and 10% soil dry weight, respectively. Then, deionized water was added to the mixtures at a water:solid ratio (W/S) of 30% and thoroughly mixed, and the mixtures were kept in a sealed polypropylene box with a cover for 7–10 days at room temperature (25 °C) (Jahandari et al. 2021; Miraki et al. 2021; Sadeghian et al. 2021). Also, deionized water was added from time to time during storage to maintain a fixed water to solid ratio. Subsequently, the Pb leaching concentration and pH of the soil were determined. The experiments were performed in triplicate.

Testing methods

The crystal morphology of PR-, APR-, and APR-adsorbed Pb product was determined using an X-ray diffraction (XRD) meter (D8 Advance, Bruker-AXS, Billerica, MA, USA) at 40 kV and 40 mA with CuKa radiation, scanning range of 10–85° in 2θ, and scanning rate of 1°/min. The data obtained were analyzed using Jade 6.5 software. The elements in PR and APR were determined by XRF analyzer (ARL 9900, Thermo Fisher Scientific, Waltham, MA, USA) at 60 kV. LiF200, LiF220, Ge111, and AX03 were selected as spectroscopic crystals. The morphology of PR-, APR-, and APR-adsorbed Pb product was observed using scanning electron microscope (SEM; S-4800, Hitachi, Tokyo, Japan) at 15-kV low accelerating voltage. The specific surface areas of PR and APR were detected by automatic specific surface area analyzer (QuadraSorb SI, Quantachrome, Boynton Beach, LA, USA). The surface functional groups of APR-adsorbed Pb product were examined by Fourier transform infrared spectrometer (FT-IR; VERTEX 70 V, Bruker, Billerica, MA, USA). Soil pH was determined using a pH meter (Delta320, Mettler-Toledo, Colombus, OH, USA) at a soil to water ratio of 1:2.5 after 1–3 h of equilibrium. The leaching concentration of Pb in soil was measured by TCLP (USEPA 2014) and inductively coupled plasma mass spectrometry (ICP-MS; Agilent 7500, Santa Clara, CA, USA).

Results and discussion

XRD analysis of PR and APR

Organic acid activation of PR

The change in the diffraction peak in the XRD patterns can reflect the crystal structure of phosphate rock (PR), with sharp diffraction peaks indicating good crystallinity and passivation of diffraction peaks denoting the existence of organic matter (Feng et al. 2008). The XRD patterns of PR and two kinds of organic acid activated PR are shown in Fig. 1. It can be noted from the figure that the main components of PR were fluorapatite ($Ca_5(PO_4)_3F$) and dolomite ($CaMg(CO_3)_2$). After activation with oxalic acid, the peak intensity of fluorapatite weakened and the peak shape widened, indicating that the crystallinity of fluorapatite decreased. Likewise, the peak intensity of dolomite was significantly weakened and the peak of calcium oxalate appeared, demonstrating that fluorapatite and dolomite dissolved to release Ca^{2+} and combined with $C_2O_4^{2-}$ in oxalic acid to form calcium oxalate monohydrate. This result is consistent with the findings of Jiang et al. (Jiang et al. 2012) and Zhang et al. (Zhang et al. 2018). The peak intensity of fluorapatite in PRC decreased but was higher than that in PRO. Furthermore, the dolomite peak disappeared and hydroxyapatite peak appeared, suggesting that fluorapatite and dolomite dissolved in citric acid to release Ca^{2+} and P elements (Ding et al. 2015; Zhang et al. 2018).

Analysis of the elements' content in PR and organic acid–activated PR (Table 1) revealed that the Ca contents in PRO and PRC decreased from 50.33 to 39.73% and 33.11%, respectively, and the P contents decreased from

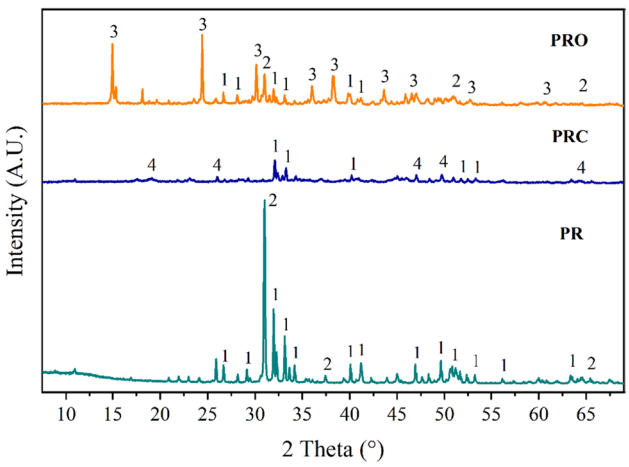

Fig. 1 XRD patterns of PR and organic acid activated PR. (1) Fluorapatite ($Ca_5(PO_4)_3F$), (2) dolomite ($CaMg(CO_3)_2$), (3) weddellite ($CaC_2O_4{\cdot}H_2O$), (4) hydroxyapatite ($Ca_5(PO_4)_3(OH)$)

Table 1 Elements content and pH of PR and organic acid activated PR

Element Sample	Ca (%)	P (%)	Mg (%)	Si (%)	F (%)	pH
PR	50.33	8.80	4.64	1.09	1.15	9.53
PRO	39.73	4.13	3.33	0.72	0.28	4.71
PRC	33.11	4.46	4.36	0.66	0.35	3.37

8.80 to 4.13% and 4.46%, respectively, which proved that the mineral components containing Ca and P in PR reacted and released active Ca and P ions. In addition, 53.07% and 49.32% of P in PR were dissolved after oxalic acid activation and citric acid activation, respectively, indicating that organic acid activation may increase the release of P in PR and that oxalic acid had stronger ability to release P in PR than citric acid. Similarly, Huang et al. (Huang et al. 2019) and Mendes et al. (Mendes et al. 2020) also reported that organic acids can promote P release from PR and increase its available P content. Furthermore, Mendes et al. (Mendes et al. 2020) suggested that the higher PR activation efficiency of oxalic acid was mainly owing to the interaction of two adjacent carboxylic groups in oxalic acid, which reduced the value of its dissociation constant ($pK_{a1} = 1.25$) to lower than that of citric acid ($pK_{a1} = 3.13$). As a result, oxalic acid was much more acidic than citric acid, with stronger ability to release P from PR.

Thermal activation of PR

The XRD patterns and main fluorapatite peaks of PR and the three kinds of thermal-activated PR are shown in Fig. 2. It can be seen from the figure that thermal activation only changed the intensity and shape of the diffraction peaks in various phases of PR, and there was no evident formation of new substance in the activation process. The intensity and shape of the fluorapatite peak changed after thermal treatment, showing a weakened peak intensity and a widened peak shape with the increase of treatment temperature.

With thermal activation, the specific surface area (SSA) of PR increased in proportion to the treatment temperature, and PR200, PR400, and PR600 presented 5.52%, 6.36%, and 43.22% higher SSA, respectively, when compared with PR. Thermal activation of PR predominantly removed the impurities and internal moisture, changed the crystal structure, and increased the SSA, resulting in an improvement in surface adsorption of Pb, which was more conducive to Pb adsorption and stability.

Thermal-organic acid activation of PR

Figure 2 shows the XRD patterns and main fluorapatite peaks of thermal-organic acid–activated PR. The peak intensity of fluorapatite in thermal-organic acid–activated PR was significantly weakened and the peak shape was broadened, when compared with that in organic acid activated PR and thermal activated PR. The peak intensity of fluorapatite in the PRO series was lower than that in the PRC series. Besides, the fluorapatite peak intensity weakened and peak shape widened with the increasing treatment temperature. These findings are consistent with the results of organic acid activation of PR and thermal activation of PR. It must be noted that the effect of organic acid activation of PR on reduction of fluorapatite peak intensity was stronger than that of thermal activation of PR.

SEM analysis of PR and APR

The results of the present study revealed that oxalic acid was more effective in activation than citric acid as it exhibited stronger ability to release P. The SSA of PR600 increased more significantly among the three thermal treatments. In the thermal-organic acid activation of PR, the effects of acid and thermal conditions on PR were consistent with those observed following acid or thermal activation of PR. Therefore, PR, PR600, PRO, and PRO-600 were selected for SEM analysis (Fig. 3). The PR presented a compact structure, good crystallinity, and large particle size. After activation, the activated phosphate rock (APR) exhibited loose structure, low crystallinity, smaller particle size, and porous structure, which increased its SSA. It has been reported that the increase in the SSA of PR owes to surface precipitation and erosion by organic acid during the activation process (Tran et al. 2015). As a result, the pore and micropore structures of APR were increased, which was conducive to physical adsorption of Pb on PR and enhanced Pb adsorption and stability (Tansel et al. 2006).

Stabilization of Pb in soil by PR and APR

The leached Pb concentrations in soil treated with PR and different kinds of APR are shown in Fig. 4. When compared with PR, APR exerted a more obvious stabilization effect on Pb-contaminated soil, with thermal-organic acid–activated PR exhibiting the best effect. The stabilization effectiveness of different kinds of APR was as follows: thermal-organic acid–activated PR > organic acid–activated PR > thermal-activated PR. With the addition of 2–10% activator, the stabilization effect of PRO was better than that of

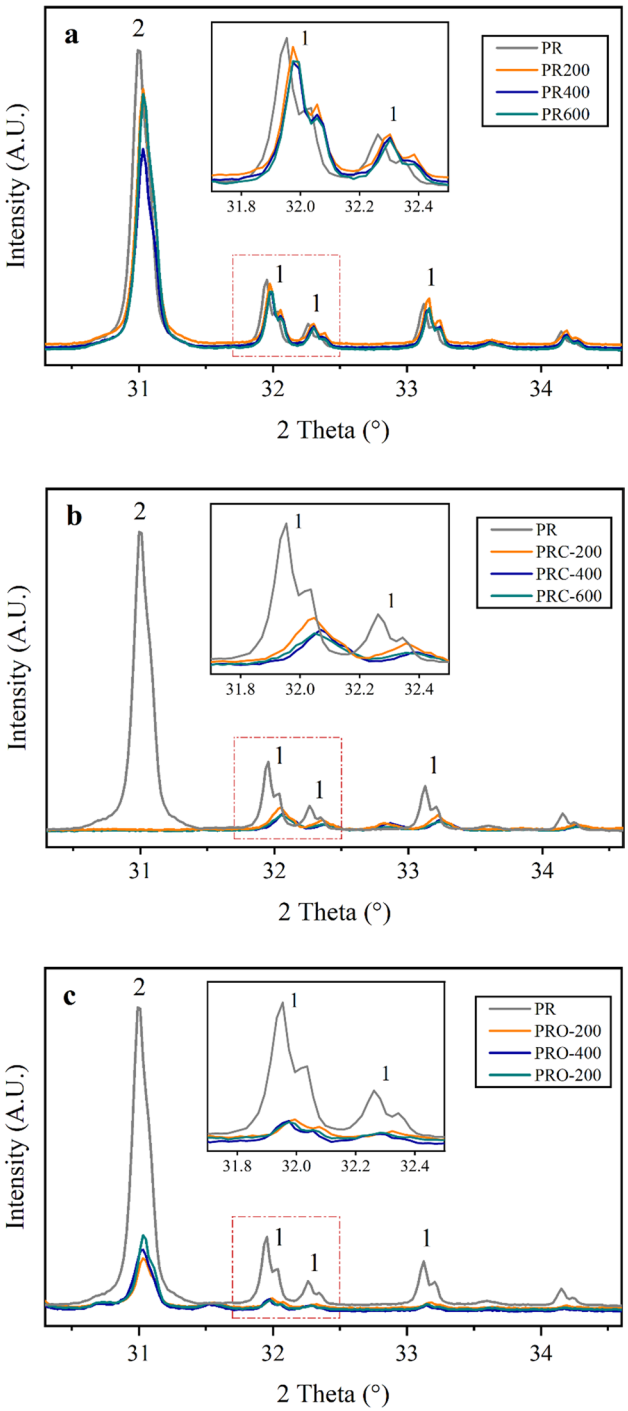

Fig. 2 XRD patterns and main fluorapatite peaks of thermal-activated PR and thermal-organic acid–activated PR (**a** thermal-activated PR, **b–c** thermal-organic acid–activated PR). (1) Fluorapatite ($Ca_5(PO_4)_3F$), (2) dolomite ($CaMg(CO_3)_2$)

PRC, and the soil Pb leaching concentration decreased by 87.1–99.1% and 29.7–78.7%, respectively. The stabilization effect of PR on Pb-contaminated soil was directly proportional to the thermal treatment temperature (200–600 °C), and the Pb leaching concentration in soil treated with PR600 decreased by 52.9–86.8%. PRO-600 exhibited the best stabilization effect, reducing Pb leaching concentration in soil by 94.0–99.8%.

The pH of the treated soil increased from 7.61 to 7.96–8.87, which may be owing to the addition of excessive PR/APR. It is presumed that PR addition to the Pb solution results in pyromorphite precipitation, releasing H^+ that could dissolve phosphate in the solution, which in turn could consume H^+. Therefore, the pH of the solution first decreased and then increased. When this dissolution–precipitation reaction reached an equilibrium, the change in the pH of the solution theoretically became 0. However, under practical conditions, excessive amounts of P-containing substances are often added, resulting in an increase in soil pH after the equilibrium reaction (Chen et al. 2010; Ma et al. 1993). Alternatively, the change in soil pH may also be related to the content of available Ca and Mg in PR/APR. Previous studies have shown that the contents of exchangeable Ca and Mg in soil presented a significant positive correlation with soil pH (Ok et al. 2011), which may be one of the reasons for the increase in soil pH with the addition of PR/APR observed in the present study. Soil pH can affect the forms of Pb that occur in soil. When the soil pH is low, a competitive relationship exists between H^+ and heavy metal ions, which leads to the inhibition of heavy metal adsorption. However, when the soil pH is high, such adsorption competition is weakened and heavy metal ions are more stable. Thus, Pb^{2+} in the soil can easily form hydroxide or phosphate precipitation/co-precipitation (Hamid et al. 2018). Chuan et al. (1996) found that the content of available Pb in soil was very low under alkaline conditions (pH = 8), and Houben et al. (2012) showed that the bioavailability of Pb in soil decreased with the increase in alkalinity. Therefore, it can be concluded that APR enhanced the stability of soil Pb by increasing the soil pH.

Recent studies have suggested that P-containing materials reduced the availability of Pb in soil mainly by varying the soil pH, adsorption, and precipitation. Precipitation reaction dominated at high pH condition compared to adsorption reaction. PR treated with acids can combine in the form of $H_2PO_4^-$ with Pb in the soil to form stable pyromorphite (Arnich et al. 2003; Chaturvedi et al. 2007; Cheyns et al. 2012) and can improve soil pH, weaken the adsorption competition between H^+ and Pb^{2+}, promote Pb^{2+} to precipitate, and reduce the mobility of Pb in soil (Huang et al. 2019). Therefore, the stability of Pb in the soil increases with the increasing amount of P released by the dissolution of PR in organic acids. As the P release ability of PRO was stronger than that of PRC because oxalic acid could more effectively promote the dissolution of PR and release P, the stabilization effect of PRO on soil Pb was more potent than that of PRC. The Pb leaching concentration in soil decreased after

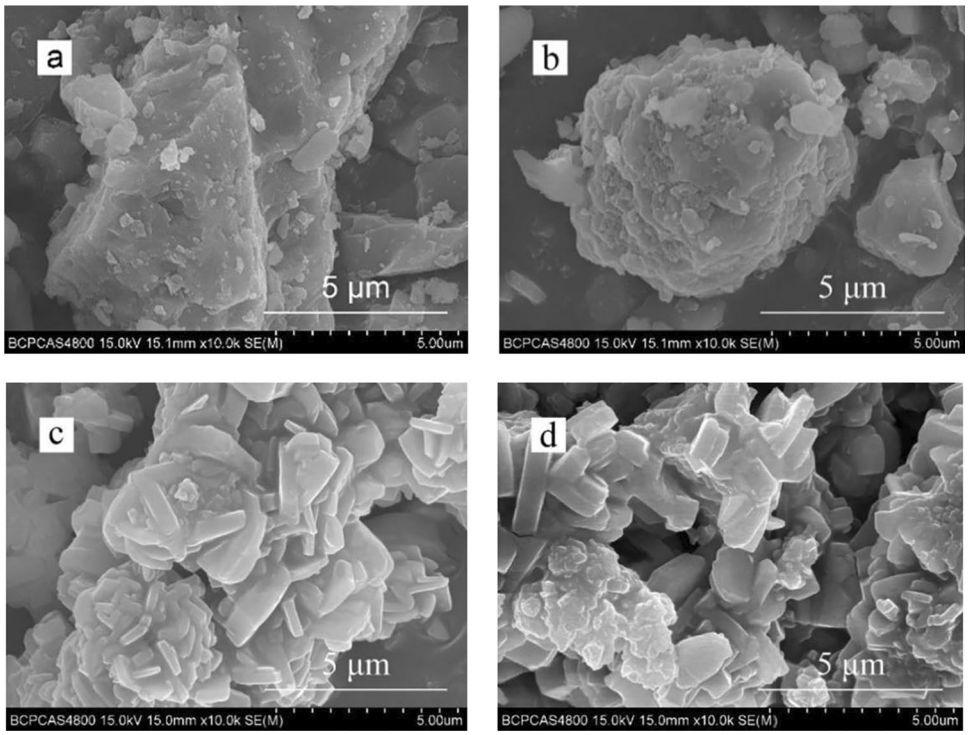

Fig. 3 SEM analysis of PR before and after activation (**a** PR, **b** PR600, **c** PRO, **d** PRO-600)

treatment with thermal activated PR, and the stabilization effect of APR on Pb in soil improved with the increasing temperature of thermal activation. This effect may be owing to the change in the structure of PR following high-temperature treatment, which increased the SSA of PR and promoted adsorption of Pb in soil by PR. The SSA of PR significantly increased with the increasing thermal activation temperature. Thus, PR600 exhibited the most significant stabilization effect. Furthermore, thermal-organic acid activation of PR showed significantly improved stabilization effect on soil Pb owing to the combined influences of organic acid activation and thermal activation. Thus, the stabilization effectiveness of APR was as follows: thermal-organic acid–activated PR > organic acid–activated PR > thermal-activated PR.

Characterization of APR-adsorbed Pb

To further verify the above-mentioned results, Pb^{2+} adsorption on PRO-600 (which presented maximum beneficial characteristics) was examined by adding $Pb(NO_3)_2$ (analytical reagent) solution to PRO-600 at a dry weight basis of 600 mg/g, and characterizing and analyzing the reaction products. The XRD patterns before and after the reaction of PRO-600 with Pb are shown in Fig. 5. Fluoropyromophite [$Pb_5(PO_4)_3F$] was detected in the products after the reaction of PRO-600 with Pb, and the peak intensity of fluorapatite weakened or even disappeared. It can be interpreted as PO_4^{3-} in PRO-600 first reacted with Pb in aqueous solution and then gradually formed $Pb_5(PO_4)_3F$ with the increase in pH, resulting in Pb immobilization. This further verified the hypothesis of dissolution–precipitation reaction between APR and Pb. Ma (1996) (Ma 1996) analyzed the products of hydroxyapatite adsorbed by Pb and found that P-Pb precipitation can occur at both high and low concentration of dissolved Pb.

The SEM/EDS analysis results of PRC-600 before and after Pb^{2+} adsorption and the mapping diagrams of typical elements are shown in Fig. 6. The SEM images revealed that PRO-600 had a rougher surface and more pores. However, after adsorption of Pb, the pores were reduced and the surface was covered with irregular particles. It must be noted that pore plugging may be detrimental to secondary adsorption. The main elements in the product after adsorption were Ca, O, Mg, P, etc. and the proportion of Pb was increased, when compared with those before adsorption, which may be owing to the formation of P-Pb compounds after Pb adsorption. Combined with the XRD results, it can be inferred that the abovementioned product was $Pb_5(PO_4)_3F$. As shown in the mapping diagram in Fig. 6, Ca and Mg in the product formed after the reaction between PRC-600 and Pb^{2+} were more loosely distributed than those before the reaction, and Pb elements appeared after the reaction, thus indicating that the cations in PRO-600 were replaced by Pb resulting in Pb adsorption.

FT-IR spectroscopy was employed to analyze the changes in the functional groups before and after the reaction between PRC-600 and Pb (Fig. 7). The FT-IR peak at 1313 cm^{-1} corresponded to the stretching peak of metal

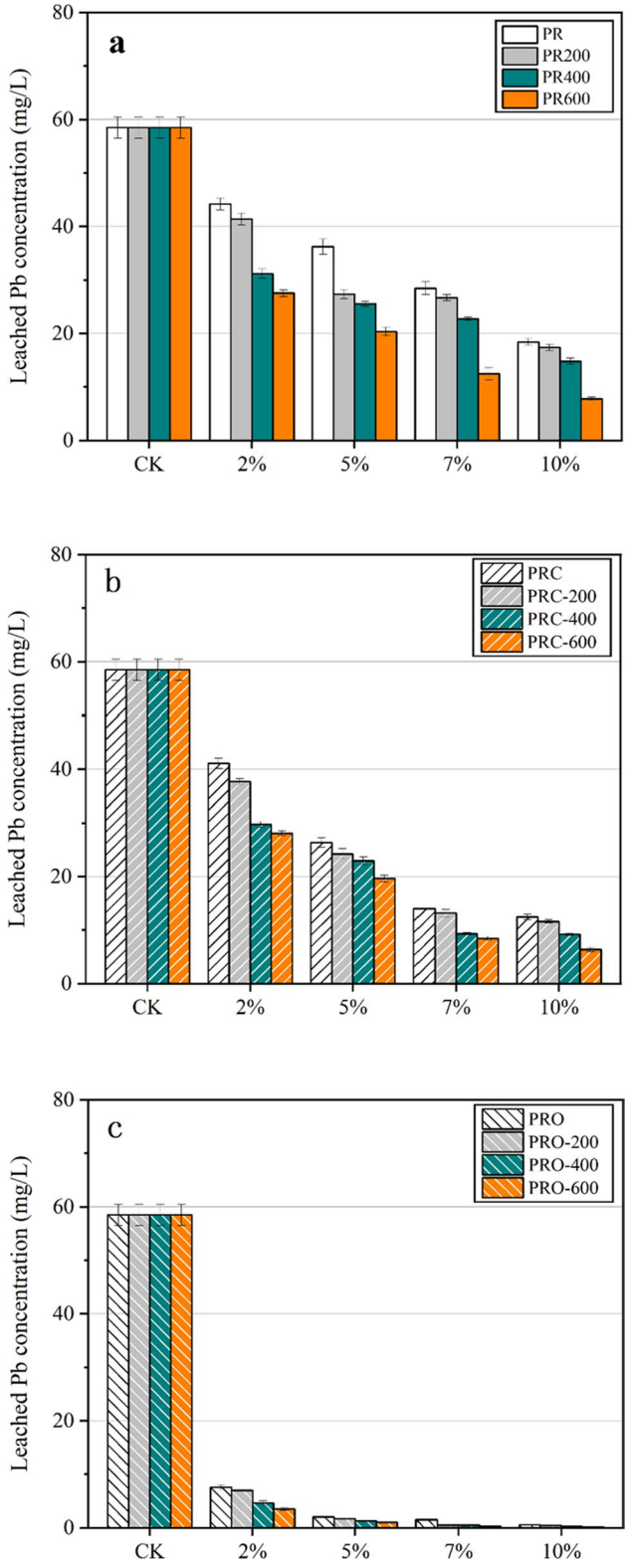

Fig. 4 Leached Pb concentrations in soil treated with PR and different kinds of activated PR (**a** PR, PR200, PR400, PR600; **b** PRC, PRC-200, PRC-400, PRC-600; **c** PRO, PRO-200, PRO-400, PRO-600) under the condition of various dry weight ratios. Error bars represent standard deviation (SD) ($n=3$) (1) Fluorapatite ($Ca_5(PO_4)_3F$), (2) dolomite ($CaMg(CO_3)_2$), (3) weddellite ($CaC_2O_4{\cdot}H_2O$), (4) fluoropyromophite ($Pb_5(PO_4)_3F$)

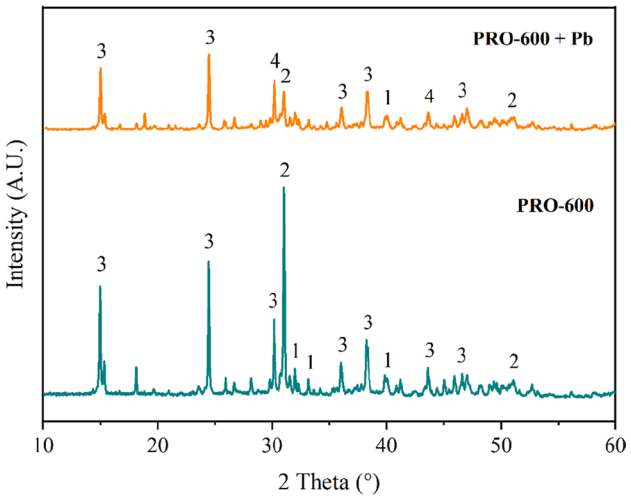

Fig. 5 XRD patterns of PRO-600 after adsorption of Pb^{2+}

carboxylate; the characteristic peak at 1616 cm^{-1} conformed to the bending vibration mode. The five peaks between 3000 cm^{-1} and 3500 cm^{-1} were consistent with the asymmetric and symmetric stretching peaks of water molecules coordinated with calcium oxalate (Ali et al. 2008). After the adsorption of Pb, the O-C-O bending vibration peak at 519 cm^{-1} shifted, and the intensity of the calcium oxalate absorption peak (1313 cm^{-1}) weakened. It implied that during the adsorption of Pb, the oxygen-containing active groups in PRO-600 were participated in the reaction, and the calcium oxalate was consumed. In addition, the absorption peaks of $H_2PO_4^-$ at 889 cm^{-1} and 958 cm^{-1} disappeared, suggesting that phosphate played an important role in the process of Pb adsorption by PRO-600. Thus, the results of XRD, SEM–EDS-mapping, and FTIR characterization of the reaction product of PRO-600 and Pb revealed that Pb^{2+} was adsorbed on APR mainly through solution-precipitation reaction to form fluoropyromophite.

Conclusions

In this study, phosphate rock (PR) was used as a raw material to examine the effectiveness of different activation methods such as organic acid activation, thermal activation, and thermal-organic acid activation, and the stabilization effects of activated phosphate rock (APR) on Pb-contaminated soil were analyzed. The results indicated that organic acid activation, thermal activation, and thermal-organic acid activation decreased the crystallinity of PR and increased the specific surface area of PR by making its structure porous. Better activation of oxalic acid than citric acid in organic acid treatment, and as for thermal treatment, the activation effect improved with the increasing treatment temperature

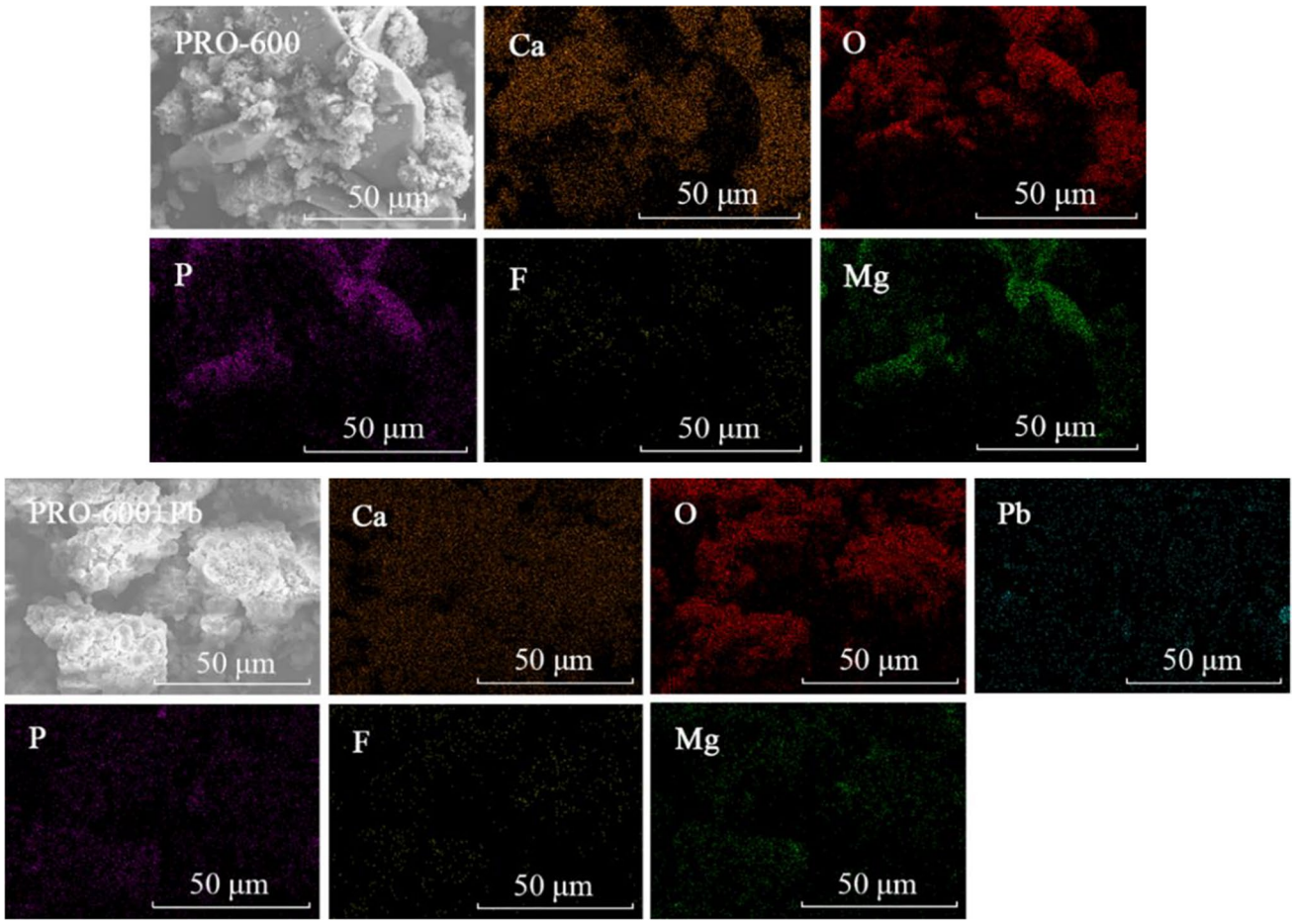

Fig. 6 SEM–EDS-mapping images of PRO-600 after adsorption of Pb^{2+}

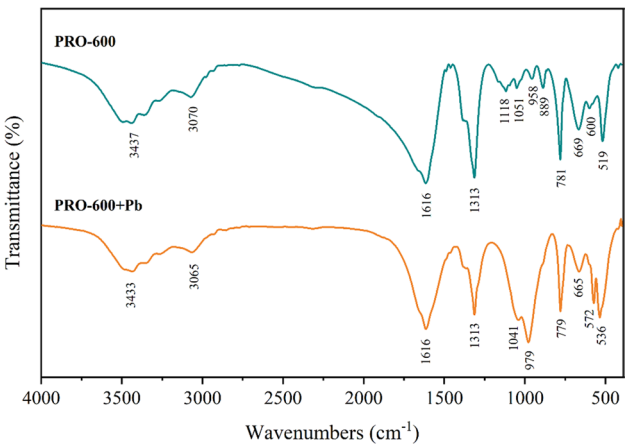

Fig. 7 FT-IR spectra of PRO-600 after adsorption of Pb^{2+}

(200–600 °C). All the three treatments enhanced the stabilization effect of PR on Pb in soil, and their effectiveness was as follows: thermal-organic acid–activated PR > organic acid–activated PR > thermal-activated PR. PRO-600 exhibited the best stabilization effect, reducing Pb leaching concentration in soil by 94.0–99.8% with the addition of 2–10% modifier, respectively. Soil Pb was stabilized mainly by the formation of fluoropyromophite precipitation with APR, which was demonstrated in the characterization of the product after Pb adsorption by PRO-600. These results suggested that thermal-organic acid–activated PR was a more efficient stabilization material for treating Pb-contaminated soil. In the practical application of APR-based remediation technology, field trials are recommended, and it is necessary to consider the existence of low-molecular-weight organic acids in the site environment. This study only considered the stabilization effect of APR on soil Pb, and the effectiveness and mechanism of APR on combined contamination of various heavy metals in soils could be the focus of further study.

Author contribution Ziwen Song: Conceptualization, experiments, data methodology, writing—original draft. Zhuo Zhang: Conceptualization, methodology, writing—review and editing. Canyu Luo: Experiments, data analysis. Likun Yang: Experiments, data recording. Jin Wu: Data analysis.

Funding This work was supported by the National Natural Science Foundation of China (Grant No. 41907131) and the Fundamental Research Funds for the Central Universities, CUGB (Grant No. 53200759566).

Data availability The data and materials used or analyzed during the current study are available from the corresponding author on reasonable request.

Declarations

Ethics approval and consent to participate Not applicable.

Consent for publication Not applicable.

Competing interests The authors declare no competing interests.

References

Abbasi MK, Manzoor M (2018) Biosolubilization of phosphorus from rock phosphate and other P fertilizers in response to phosphate solubilizing bacteria and poultry manure in a silt loam calcareous soil. J Plant Nutr Soil Sci 181:345–356

Ali AM, Nambi Raj NA, Kalainathan S, Palanichamy P (2008) Microhardness and acoustic behavior of calcium oxalate monohydrate urinary stone. Mater Lett 62:2351–2354

Arnich N, Lanhers MC, Laurensot F, Podor R, Montiel A, Burnel D (2003) In vitro and in vivo studies of lead immobilization by synthetic hydroxyapatite. Environ Pollut 124:139–149

Awa SH, Hadibarata T (2020): Removal of heavy metals in contaminated soil by phytoremediation mechanism: a review. Water, Air, Soil Pollut. 231

Chaturvedi PK, Seth CS, Misra VJJOHM (2007) Selectivity sequences and sorption capacities of phosphatic clay and humus rich soil towards the heavy metals present in zinc mine tailing. J Hazard Mater 147:698–705

Chen SB, Li N, Wang M, Wei DP (2010) Factors needed to be reconsidered during in-situ remediation practices of Pb-polluted soils with P. Chin J Eco-Agric 18:203–209

Cheyns K, Peeters S, Delcourt D, Smolders E (2012) Lead phytotoxicity in soils and nutrient solutions is related to lead induced phosphorus deficiency. Environ Pollut 164:242–247

Chowdhury KIA, Nurunnahar S, Kabir ML, Islam MT, Forsyth JE (2021) Child lead exposure near abandoned lead acid battery recycling sites in a residential community in Bangladesh: Risk factors and the impact of soil remediation on blood lead levels. Environ Res 194:110689

Chuan MC, Shu GY, Liu JC (1996) Solubility of heavy metals in a contaminated soil: Effects of redox potential and pH. Water, Air, Soil Pollut 90:543–556

Ding ZL, Zhao L, Xu XY, Luo QS, Cao XD (2015) Enhanced immobilization of Pb / Zn in compound contaminated soil by modified natural phosphate rock. Environ Chem 34:1049–1056

Feng ZB, Liu XM, Liu GR, Zou SW, Zhang SQ, Zhang JF, Wang YJ, Zhang FD (2008) Preparation and testing of two kinds of modified phosphorite powder. Plant Nutr Fert Sci 14:792–796

Gottesfeld P, Were FH, Adogame L, Gharbi S, San D, Nota MM, Kuepouo G (2018) Soil contamination from lead battery manufacturing and recycling in seven African countries. Environ Res 161:609–614

Hamid Y, Tang L, Wang X, Hussain B, Yaseen M, Aziz MZ, Yang X (2018) Immobilization of cadmium and lead in contaminated paddy field using inorganic and organic additives. Sci Rep 8:17839

Houben D, Pircar J, Sonnet P (2012) Heavy metal immobilization by cost-effective amendments in a contaminated soil: effects on metal leaching and phytoavailability. J Geochem Explor 123:87–94

Huang GY, Gao RL, You JW, Zhu J, Fu QL, Hu HQ (2019) Oxalic acid activated phosphate rock and bone meal to immobilize Cu and Pb in mine soils. Ecotoxicol Environ Saf 174:401–407

Jahandari S, Mohammadi M, Rahmani A, Abolhasani M, Miraki H, Mohammadifar L, Kazemi M, Saberian M, Rashidi M (2021) Mechanical properties of recycled aggregate concretes containing silica fume and steel fibres. Materials 14:7065

Jiang GJ, Liu YH, Huang L, Fu QL, Deng YJ, Hu HQ (2012) Mechanism of lead immobilization by oxalic acid-activated phosphate rocks. J Environ Sci 24:919–925

Kumpiene J, Lagerkvist A, Maurice C (2008) Stabilization of As, Cr, Cu, Pb and Zn in soil using amendments–a review. Waste Manage 28:215–225

Li QQ, Zhong HQ, Cao Y (2020) Effects of the joint application of phosphate rock, ferric nitrate and plant ash on the immobility of As, Pb and Cd in soils. J Environ Manage 265:110576

Ma LQ (1996) Factors influencing the effectiveness and stability of aqueous lead immobilization by hydroxyapatite. J Environ Qual 25:1420–1429

Ma QY, Traina SJ, Logan TJ, Ryan JA (1993) In situ lead immobilization by apatite. Environ Sci Technol 27:1803–1810

Mendes GDO, Murta HM, Valadares RV, da Silveira WB, Silva IR, Costa MD (2020) Oxalic acid is more efficient than sulfuric acid for rock phosphate solubilization. Miner. Eng. 155:106458

Mignardi S, Corami A, Ferrini V (2012) Evaluation of the effectiveness of phosphate treatment for the remediation of mine waste soils contaminated with Cd, Cu, Pb, and Zn. Chemosphere 86:354–360

Miraki H, Shariatmadari N, Ghadir P, Jahandari S, Tao Z, Siddique R (2021): Clayey soil stabilization using alkali-activated volcanic ash and slag. J. Rock Mech. Geotech. Eng.

Ok YS, Lim JE, Moon DH (2011) Stabilization of Pb and Cd contaminated soils and soil quality improvements using waste oyster shells. Environ Geochem Health 33:83–91

E.Padilla-Ortega, N.Medellín-Castillo, A.Robledo-Cabrera (2020): Comparative study of the effect of structural arrangement of clays in the thermal activation: evaluation of their adsorption capacity to remove Cd(II). J. Environ. Chem. Eng. 8

Park JH, Bolan N, Megharaj M, Naidu R (2011) Comparative value of phosphate sources on the immobilization of lead, and leaching of lead and phosphorus in lead contaminated soils. Sci Total Environ 409:853–860

Sadeghian F, Jahandari S, Haddad A, Rasekh H, Li J (2021): Effects of variations of voltage and pH value on the shear strength of soil and durability of different electrodes and piles during electrokinetic phenomenon. J. Rock Mech. Geotech. Eng.

Su XJ, Zhu J, Fu QL, Zuo JC, Liu YH, Hu HQ (2015) Immobilization of lead in anthropogenic contaminated soils using phosphates with/without oxalic acid. J Environ Sci 28:64–73

Tansel B, Sager J, Rector T, Garland J, Strayer RF, Levine L, Roberts M, Hummerick M, Bauer J (2006) Significance of hydrated radius and hydration shells on ionic permeability during nanofiltration in dead end and cross flow modes. Sep Purif Technol 51:40–47

Tran L, Wu PX, Yang L, Zhu YJ, Huang ZJ (2015) Characteristics of organic modified vermiculites and the adsorption of Hg^{2+}. Acta Sci Circumst 35:1054–1060

USEPA (2014): SW-846 Test Method 1314: Liquid-solid partitioning as a function of liquid-solid ratio for constituents in solid materials using an up-flow percolation column procedure

Xu D, Liu SQ, Yao YQ, Liu HL, Pei Y (2017) A review on new technological progress for beneficiation of refractory phosphate ore in China. IOP Conf Ser Earth Environ Sci 63:012043

Xu JC, Huang LM, Chen CY, Wang J, Long XX (2019) Effective lead immobilization by phosphate rock solubilization mediated by phosphate rock amendment and phosphate solubilizing bacteria. Chemosphere 237:124540

Yan YB, Li Q, Yang JJ, Zhou SY, Wang LJ, Bolan N (2020) Evaluation of hydroxyapatite derived from flue gas desulphurization gypsum on simultaneous immobilization of lead and cadmium in contaminated soil. J. Hazard. Mater. 400:123038

Yao ZT, Li JH, Xie HH, Yu CH (2012) Review on Remediation Technologies of Soil Contaminated by Heavy Metals. Procedia Environ Sci 16:722–729

Zhang Z, Guo GL, Teng YG, Wang JS, Rhee JS, Wang S, Li FS (2015) Screening and assessment of solidification/stabilization amendments suitable for soils of lead-acid battery contaminated site. J Hazard Mater 288:140–146

Zhang Z, Guo GL, Wang M, Zhang J, Wang ZX (2018) Enhanced stabilization of Pb, Zn, and Cd in contaminated soils using oxalic acid-activated phosphate rocks. Environ Sci Pollut Res 25:2861–2868

Zhou F, Ye GY, Gao YT, Wang HQ, Zhou S, Liu Y, Yan CJ (2022) Cadmium adsorption by thermal-activated sepiolite: Application to in-situ remediation of artificially contaminated soil. J. Hazard. Mater. 423:127104

Zhu J, Cai ZJ, Su XJ, Fu QL, Liu YH, Huang QY, Violante A, Hu HQ (2015) Immobilization and phytotoxicity of Pb in contaminated soil amended with γ-polyglutamic acid, phosphate rock, and γ-polyglutamic acid-activated phosphate rock. Environ Sci Pollut Res 22:2661–2667